

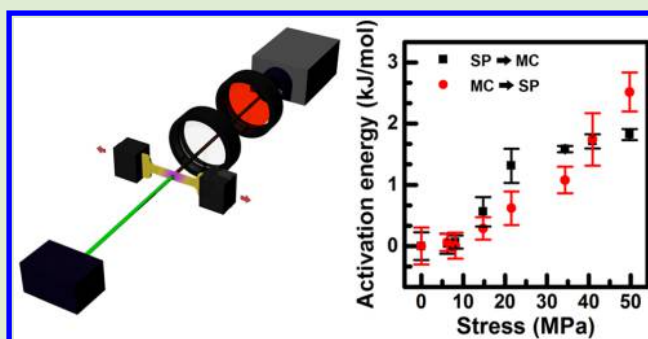
# Effect of Mechanical Stress on Spiropyran-Merocyanine Reaction Kinetics in a Thermoplastic Polymer

Tae Ann Kim,<sup>†,‡</sup> Brett A. Beiermann,<sup>†,‡</sup> Scott R. White,<sup>‡,§</sup> and Nancy R. Sottos<sup>\*,†,‡</sup>

<sup>†</sup>Department of Materials Science and Engineering, <sup>‡</sup>Beckman Institute of Advanced Science and Technology, and <sup>§</sup>Aerospace Engineering, University of Illinois at Urbana–Champaign, Urbana, Illinois 61801, United States

## Supporting Information

**ABSTRACT:** Mechanical force alters the potential energy surface of a mechanophore reaction by modifying the activation energy for conversion. The effects of force on the rate constants and activation energies are not well characterized for mechanophores in bulk polymers. In this work, spiropyran-linked polyurethanes are synthesized and the kinetics of the spiropyran-merocyanine transition in the bulk polymer measured under different values of a macroscopic tensile stress. Above a critical threshold stress, the forward rate constant (spiropyran to merocyanine transition) increases, while the reverse rate constant (merocyanine to spiropyran transition) decreases with applied stress. A tensile stress of 50 MPa enhances the forward rate constant by 110% and lowers the forward activation energy by 1.8 kJ/mol compared to the unstressed condition. Also, this same amount of stress reduces the reverse rate constant by 65% and increases the reverse activation energy by 2.5 kJ/mol.



Mechanical force can trigger desirable chemical transitions in mechanophore-linked polymers. Mechanophores are force-sensitive molecules that are integrated into a polymer within a solution or a solid state. Mechanophore-linked polymers can exhibit mechanically induced color change, which can be used for imaging stress/strain distributions or damage detection.<sup>1–5</sup> Other mechanochemical functions include force-induced catalysis and polymerization,<sup>6–8</sup> small molecule release,<sup>9,10</sup> and cross-linking.<sup>11,12</sup> Also, thermally or photochemically prohibited reactions have been achieved mechanically, implying that mechanical force can modify the potential energy surface of certain reactions.<sup>13–15</sup>

The effect of mechanical force on the kinetics of chemical reactions has mainly been investigated for single-molecule systems. Wiita et al.<sup>16</sup> studied the effect of force on the kinetics of thiol/disulfide exchange with single-molecule force-clamp spectroscopy. Kersey et al.<sup>17</sup> compared dynamic single-molecule force spectroscopy behavior and stress-free kinetic data for well-characterized bimolecular reactions. Both studies revealed a logarithmic dependence of the kinetics on the applied force. Using a stiff stilbene molecular probe, Yang et al.<sup>18</sup> found an exponential dependence of C–C bond dissociation rate on the restoring force.

Spiropyran (SP) is a well-studied mechanophore, which undergoes a force-induced reversible  $6\pi$  electrocyclic ring opening reaction to a merocyanine (MC) form. Prior investigation of the isomerization kinetics between SP and MC under thermal and photochemical activation indicates a first-order process.<sup>19</sup> Gossweiler et al.<sup>20</sup> characterized the force-rate relationship of two SP isomers using atomic force

microscopy. Lee et al. studied the effect of stress on the equilibrium of SP–MC transition in a bulk polymer.<sup>21</sup> They showed indirect evidence that applied stress alters the potential energy surface toward the more favored MC state. The time constant for the reverse reaction (MC → SP) was retarded under applied load compared to the no-stress condition. However, this polymer required prestretching to increase chain alignment and enable mechanical activation of SP under subsequent loading. Also, only a single deformation ratio (stretch),  $\lambda = 2$  (defined as instantaneous sample gage length divided by the undeformed gage length), was compared to the initial state ( $\lambda = 1$ ).

In this study, we examine the SP–MC reaction kinetics in a SP-linked polyurethane (SP-PU) system using transition state theory (TST). Mechanically induced molecular-level processes such as viscous flow, dislocation motion and polymer yielding, wherein the stress reduces the energy barrier for molecular motion and flow, have been effectively modeled with TST.<sup>22–24</sup> Through combined mechanical and optical characterization, we calculate rate constants and activation energy for the forward and reverse reactions of SP in a bulk polymer.

SP-PU (Figure 1) was synthesized by methods reported previously,<sup>21</sup> but with a different polyethylene glycol (PEG) soft segment (see Supporting Information). The number-averaged molecular weight was 20500 g mol<sup>-1</sup> and dispersity

Received: October 26, 2016

Accepted: November 7, 2016

Published: November 11, 2016

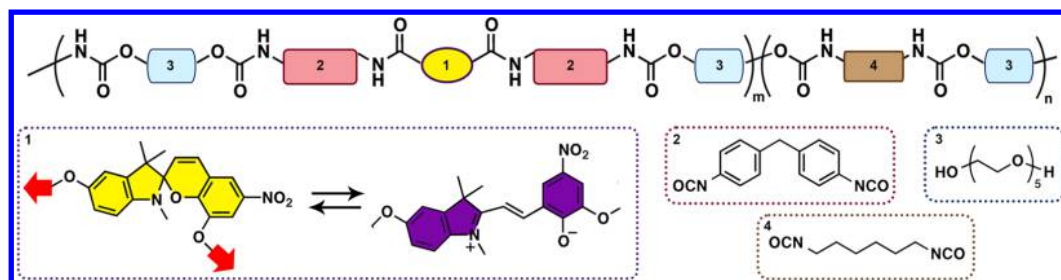


Figure 1. Chemical structure of synthesized SP-integrated PU polymer.

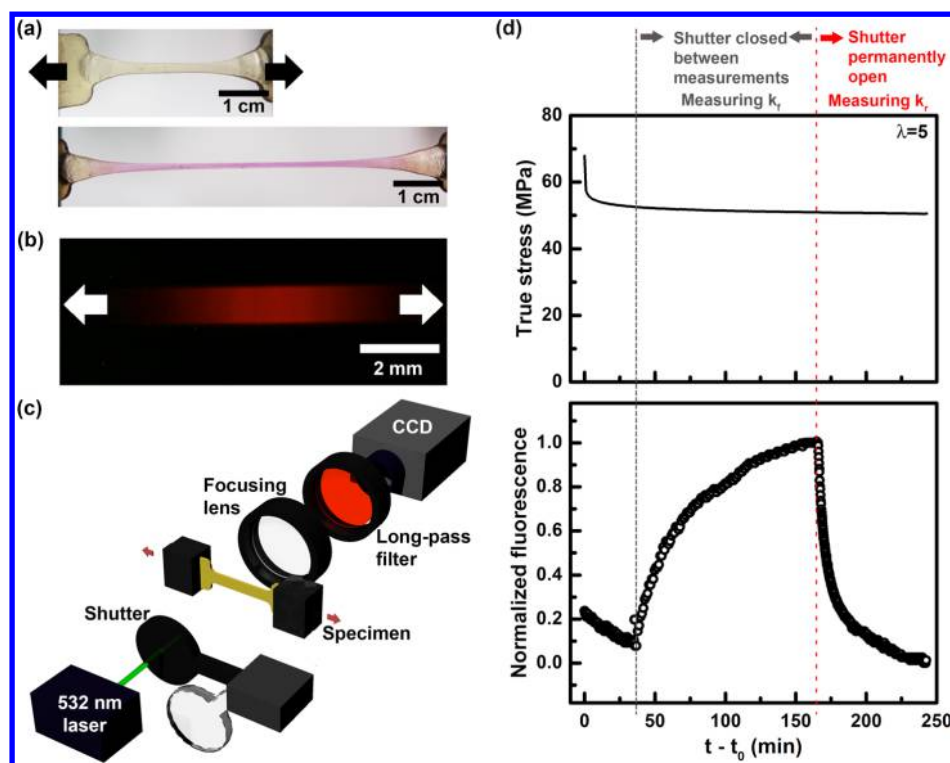


Figure 2. Observation of SP–MC conversion under constant deformation. (a) Optical images of SP-PU dog-bone before (top) and after stretching (bottom). (b) Fluorescence images of SP-PU after activation. (c) Mechanical and optical testing setup for characterization of reaction kinetics. The shutter prevents continuous bleaching between the forward reaction rate measurements. (d) True stress at constant deformation ratio ( $\lambda = 5$ ) and normalized fluorescence intensity (fluorescence signals at each time divided by the maximum fluorescence intensity,  $I/I_{\max}$ ) as a function of time ( $t_0$  denotes the time when the deformation ratio reaches a constant value). All fluorescence measurements were acquired under dark conditions.

( $\bar{D}$ ) 1.74, confirmed by gel permeation chromatography. Under no stress, the initially colorless SP-PU specimens changed to colored MC states when kept in the dark (Figure S1 in the Supporting Information). This effect was not observed in prior SP-poly(methyl acrylate)<sup>25</sup> or SP-poly(methyl methacrylate) polymers.<sup>26</sup> The equilibrium of photochromic materials such as SP is influenced by polarity of the environment due to the different polarity of the equilibrium components. Polar MC becomes more stabilized in a polar environment not only in solution but also within a polymer matrix,<sup>27</sup> implying that the PU in the current work serves as a polar medium for stabilizing MC.

Monotonic tensile loading of the SP-PU converts the SP to MC, leading to a distinct purple color change (Figure 2a). The MC also has a strong fluorescence as shown in Figure 2b. An increase in fluorescence intensity is used to detect conversion of SP to MC. A representative stress–deformation ratio curve along with the corresponding change in fluorescence intensity is included in the Supporting Information (Figure S2). The PU

has a low yield point ( $\lambda = 1.1$ ), followed by strain hardening at higher deformation ratios. Consistent with prior studies,<sup>28</sup> activation of SP occurs after the yield point.

The forward reaction (from SP to MC) rate constant is measured with a combined mechanical and optical testing setup (Figure 2c).<sup>25</sup> A low power 532 nm green laser (Crystal laser, 2.5 mW) served as an excitation light source for measuring MC fluorescence. Activated MC in the PU tensile specimens absorbs the green light and emits red fluorescence at approximately 610 nm. A long-pass fluorescence emission filter, excluding shorter wavelengths than 580 nm, enabled capture of fluorescence images by color CCD. With this setup, SP-PU dog-bones were loaded to a constant deformation ratio and then exposed to the green laser for 30 min to convert the MC back to SP form. Figure 2d shows the response of true stress and fluorescence intensity change with the constant deformation ratio (stretch),  $\lambda = 5$ , as a function of time. After 30 min (denoted by the vertical gray line in Figure 2d), fluorescence images were captured every 1 min under dark

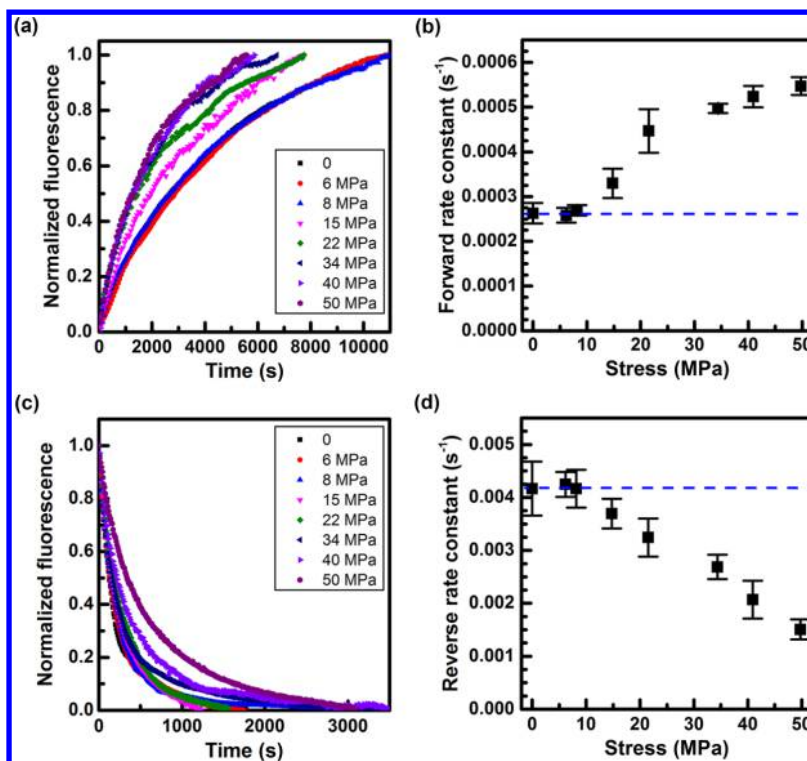


**Figure 3.** Characterization of forward and reverse rate constants for SP-linked PU. (a) Evolution of fluorescence intensity for different stress values. (b) Forward rate constant ( $k_f$ ) calculated at different applied stress values. (c) Fluorescence decay at different stress values. (d) Calculated reverse rate constant ( $k_r$ ) depending on the applied stress. Blue dashed lines indicate the initial rate constant. Error bars represent one standard deviation of the data.

conditions. To minimize photobleaching of the MC from the excitation source, a mechanical shutter was placed in front of the light source and temporarily open only when taking images. After the fluorescence intensity reached a constant value (denoted by the red vertical line in Figure 2d), the shutter was opened, causing the MC to revert to SP by continuous exposure of the green laser. A similar procedure was used for measuring decaying fluorescence intensity.

We also characterized the stress relaxation behavior of the SP-PU at different deformation ratios (see Figure S6 in the Supporting Information). Stress relaxation data were fit to a generalized Maxwell model (Table S1). The average relaxation times for each Maxwell element were 0.54, 17, and 290 min, respectively, which were not altered significantly at different deformation ratios. We found that approximately 20% of the initial stress relaxed within 25 min but then quickly leveled out. We calculate the average stress in this plateau region. Although the stress continues to relax slowly, it varies by at most 3.5% from the average value during the measurements. Although in this study we only measure the macroscopic stress, we previously developed multiscale computational analyses to investigate the local force felt by the SP mechanophores in glassy and rubbery polymers. We found that the macroscopic stress response can be effectively interpreted in terms of MD polymer microscale force transmission.<sup>29,30</sup>

The fluorescence intensity change at the different deformation ratios is plotted in Figure 3a. At stress levels 0, 6, and 8 MPa, the increase of the fluorescence intensity with time is nearly identical. At stress levels greater than 8 MPa, the fluorescence intensity increases more rapidly with applied stress. Since the SP–MC transition is a unimolecular reaction and the MC to SP transition is negligible under dark conditions

(see Figure S4), the kinetics of SP activation can be described by<sup>31</sup>

$$[\text{MC}(t)] = [\text{SP}]_0(1 - \exp(-k_f t)) \quad (1)$$

where  $[\text{MC}(t)]$  is MC concentration at a certain time  $t$ ,  $[\text{SP}]_0$  is the initial concentration of SP, and  $k_f$  is forward rate constant. The rate constants at each stress value are extracted by fitting the measured data to eq 1. The stress-free forward rate constant ( $k_{0,f}$ ) obtained from our measurement is  $2.6 \times 10^{-4} \text{ s}^{-1}$ , which is higher than the  $k_{0,f}$  of SP reported previously by Gossweiler et al.<sup>20</sup> We hypothesize that this difference in rates is due to the bulk PU matrix, which provides a more polar environment to stabilize the MC form. As shown in Figure 3b, a continuous increase in the forward rate constant occurs above a threshold stress of 8 MPa.

Fluorescence intensity decay during the reverse reaction is plotted in Figure 3c. During the fluorescence decay measurement, the green laser light provided additional energy to drive the reverse (MC  $\rightarrow$  SP) reaction such that the forward reaction was considered negligible (Figure S4). Similar to the case of the forward reaction, fluorescence intensity decay is retarded as higher stress is applied above a threshold value of 8 MPa. We obtain the reverse rate constant as a function of relaxation stress by fitting the results to a single-exponential decay equation,<sup>31</sup>

$$[\text{MC}(t)] = [\text{MC}]_0 \exp(-k_r t) \quad (2)$$

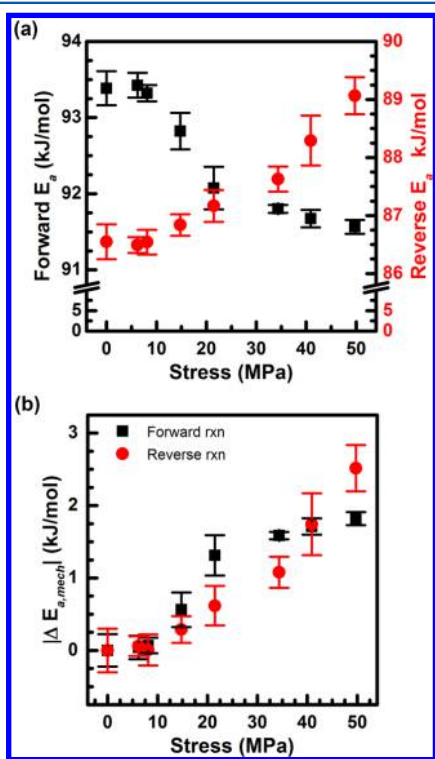
where  $[\text{MC}]_0$  and  $k_r$  are the initial concentration of MC and a reverse rate constant. As shown in Figure 3d, there is no noticeable change in the reverse rate constants below a stress of 8 MPa. Above this threshold stress value, the reverse rate constants decrease with increasing stress.

Figure S5 shows the change in normalized fluorescence intensity for varying deformation ratios. Above the threshold stress, further increase in applied stress (or deformation ratio) retards the MC  $\rightarrow$  SP transition. This effect has been observed previously for other photochromophores.<sup>32</sup> Based on prior data,<sup>25,33</sup> we hypothesize that the threshold stress is associated with the uncoiling and aligning polymer chains. Preferential activation of mechanophores occurs when the polymer chains are aligned along the tensile loading direction.<sup>34</sup>

According to the Eyring-Polanyi equation, the reaction rate constant,  $k$ , depends on activation energy  $\Delta E_a$ .<sup>35,36</sup>

$$k = \frac{k_b T}{\hbar} \exp\left(-\frac{\Delta E_a}{k_b T}\right) \quad (3)$$

where  $k_b$  is Boltzmann constant,  $\hbar$  is Planck's constant, and  $T$  is temperature. The forward and reverse activation energies calculated from eq 3 are plotted in Figure 4a. As expected,



**Figure 4.** Effect of stress on activation energy for SP–MC transition in PU. (a) Total activation energy for both the forward and reverse reaction for different applied stress levels. (b) Change in mechanical activation energy relative to zero initial stress. Error bars represent one standard deviation of the data.

applied mechanical stress lowers the activation energy for the forward reaction, indicating MC states are more favorable with higher stress. Tensile stress also increases the activation energy for the reverse reaction so that MC states are less favorable. This result is consistent with prior reports that applied force modifies the potential energy surface by decreasing the activation energy barrier for mechanophore conversion.<sup>37,38</sup>

By assuming the change we observe in total activation energy for the forward and reverse reactions is primarily due to the mechanical contribution to activation energy in our experiments, we can simplify eq 3 as follows,

$$k = k_{\sigma=0} \exp\left(-\frac{\Delta E_{mech}}{k_b T}\right) \quad (4)$$

where  $k_{\sigma=0}$  is rate constant under no stress and  $\Delta E_{mech}$  is activation energy change due to the applied mechanical load.

At small values of activation energy, the exponential term in eq 4 is approximated as linear and the activation energy is assumed a linear function of applied tensile stress,  $\sigma$ , yielding the following form of the rate equation:<sup>39,40</sup>

$$k \approx k_{\sigma=0} \left(1 - \frac{\sigma v^*}{k_b T}\right) \quad (5)$$

where  $v^*$  is the activation volume. The absolute change of the forward and reverse activation energies calculated from eq 5 for different levels of applied stress is summarized in Figure 4b. The activation energies increase with applied stress above a threshold value of 8 MPa. At stress levels of 50 MPa, the energy barrier for the transition from SP to MC decreased by 1.8 kJ/mol. For the reverse reaction from MC to SP, the same stress increased the activation energy by 2.5 kJ/mol. The corresponding average activation volumes calculated for each reaction were  $1.0 \times 10^{-1} \text{ nm}^3$  (forward) and  $4.4 \times 10^{-2} \text{ nm}^3$  (reverse). The activation volume is associated with the volumetric change between the activated state and nonactivated state.<sup>29,36,41</sup> By assuming cubic symmetry, characteristic lengths ( $d^* = (v^*)^{1/3}$ ) of 0.46 and 0.35 nm, were calculated for the forward and reverse reactions, respectively. Interestingly, prior molecular dynamic simulations and experiments,<sup>1,29,30,42</sup> estimate that  $d^*$  is on the order of  $10^{-1} \text{ nm}$  for both forward and reverse transition in SP.

In summary, we characterized the kinetics of the SP–MC transition in thermoplastic polyurethanes by measuring the fluorescence change due to activation of the mechanophores. Both forward and reverse rate constants were calculated under different applied stress values. Below a critical stress level, there was no change in the reaction kinetics. At stresses above this threshold value, the forward rate constants increased linearly with the applied stress and the reverse rate constants decreased linearly with the stress. The activation energies for both reactions were calculated as a function of applied stress. We found that the applied force lowers the activation energy for forward transition but increases the barrier for reverse reaction.

## ■ ASSOCIATED CONTENT

### 📄 Supporting Information

The Supporting Information is available free of charge on the ACS Publications website at DOI: 10.1021/acsmacrolett.6b00822.

General experimental details, description of fluorescence measurement, engineering stress–deformation ratio behavior with fluorescence change, stress relaxation behavior, and derivation of equations and their fitting results (PDF).

## ■ AUTHOR INFORMATION

### Corresponding Author

\*E-mail: n-sottos@illinois.edu.

### Notes

The authors declare no competing financial interest.

## ACKNOWLEDGMENTS

This work was supported by a grant from the National Science Foundation; Grant No. DMR 13-07354. T.A.K. acknowledges the Kwanjeong Educational foundation for a fellowship.

## REFERENCES

- (1) Davis, D. A.; Hamilton, A.; Yang, J.; Cremar, L. D.; Van Gough, D.; Potisek, S. L.; Ong, M. T.; Braun, P. V.; Martinez, T. J.; White, S. R.; Moore, J. S.; Sottos, N. R. *Nature* **2009**, *459*, 68–72.
- (2) Zhang, H.; Chen, Y.; Lin, Y.; Fang, X.; Xu, Y.; Ruan, Y.; Weng, W. *Macromolecules* **2014**, *47*, 6783–6790.
- (3) Wang, Q.; Gossweiler, G. R.; Craig, S. L.; Zhao, X. *Nat. Commun.* **2014**, *5*, 4899.
- (4) Imato, K.; Irie, A.; Kosuge, T.; Ohishi, T.; Nishihara, M.; Takahara, A.; Otsuka, H. *Angew. Chem., Int. Ed.* **2015**, *54*, 6168–6172.
- (5) Gossweiler, G. R.; Hewage, G. B.; Soriano, G.; Wang, Q.; Welshofer, G. W.; Zhao, X.; Craig, S. L. *ACS Macro Lett.* **2014**, *3*, 216–219.
- (6) Piermattei, A.; Karthikeyan, S.; Sijbesma, R. P. *Nat. Chem.* **2009**, *1*, 133–137.
- (7) Jakobs, R. T. M.; Ma, S.; Sijbesma, R. P. *ACS Macro Lett.* **2013**, *2*, 613–616.
- (8) Groote, R.; Jakobs, R. T. M.; Sijbesma, R. P. *Polym. Chem.* **2013**, *4*, 4846–4859.
- (9) Larsen, M. B.; Boydston, A. J. *J. Am. Chem. Soc.* **2013**, *135*, 8189–8192.
- (10) Diesendruck, C. E.; Steinberg, B. D.; Sugai, N.; Silberstein, M. N.; Sottos, N. R.; White, S. R.; Braun, P. V.; Moore, J. S. *J. Am. Chem. Soc.* **2012**, *134*, 12446–12449.
- (11) Wang, J.; Piskun, I.; Craig, S. L. *ACS Macro Lett.* **2015**, *4*, 834–837.
- (12) Zhang, H.; Gao, F.; Cao, X.; Li, Y.; Xu, Y.; Weng, W.; Boulatov, R. *Angew. Chem., Int. Ed.* **2016**, *55*, 3040–3044.
- (13) Stöttinger, S.; Hinze, G.; Diezemann, G.; Oesterling, I.; Müllen, K.; Basché, T. *Nat. Nanotechnol.* **2014**, *9*, 182–186.
- (14) Hickenboth, C. R.; Moore, J. S.; White, S. R.; Sottos, N. R.; Baudry, J.; Wilson, S. R. *Nature* **2007**, *446*, 423–427.
- (15) Wang, J.; Kouznetsova, T. B.; Niu, Z.; Ong, M. T.; Klukovich, H. M.; Rheingold, A. L.; Martinez, T. J.; Craig, S. L. *Nat. Chem.* **2015**, *7*, 323–327.
- (16) Wiita, A. P.; Ainavarapu, S. R. K.; Huang, H. H.; Fernandez, J. M. *Proc. Natl. Acad. Sci. U. S. A.* **2006**, *103*, 7222–7227.
- (17) Kersey, F. R.; Yount, W. C.; Craig, S. L. *J. Am. Chem. Soc.* **2006**, *128*, 3886–3887.
- (18) Yang, Q.-Z.; Huang, Z.; Kucharski, T. J.; Khvostichenko, D.; Chen, J.; Boulatov, R. *Nat. Nanotechnol.* **2009**, *4*, 302–306.
- (19) Klajn, R. *Chem. Soc. Rev.* **2014**, *43*, 148–184.
- (20) Gossweiler, G. R.; Kouznetsova, T. B.; Craig, S. L. *J. Am. Chem. Soc.* **2015**, *137*, 6148–6151.
- (21) Lee, C. K.; Davis, D. A.; White, S. R.; Moore, J. S.; Sottos, N. R.; Braun, P. V. *J. Am. Chem. Soc.* **2010**, *132*, 16107–16111.
- (22) Hoffman, J. D.; Williams, G.; Passaglia, E. *J. Polym. Sci., Part C: Polym. Symp.* **1966**, *14*, 173–235.
- (23) Kauzmann, W.; Eyring, H. *J. Am. Chem. Soc.* **1940**, *62*, 3113–3125.
- (24) Li, J. *MRS Bull.* **2007**, *32*, 151–159.
- (25) Beiermann, B. A.; Kramer, S. L. B.; May, P. A.; Moore, J. S.; White, S. R.; Sottos, N. R. *Adv. Funct. Mater.* **2014**, *24*, 1529–1537.
- (26) Beiermann, B. A.; Davis, D. A.; Kramer, S. L. B.; Moore, J. S.; Sottos, N. R.; White, S. R. *J. Mater. Chem.* **2011**, *21*, 8443–8447.
- (27) Such, G.; Evans, R. A.; Yee, L. H.; Davis, T. P. *J. Macromol. Sci., Polym. Rev.* **2003**, *43*, 547–579.
- (28) Kingsbury, C. M.; May, P. A.; Davis, D. A.; White, S. R.; Moore, J. S.; Sottos, N. R. *J. Mater. Chem.* **2011**, *21*, 8381–8388.
- (29) Silberstein, M. N.; Min, K.; Cremar, L. D.; Degen, C. M.; Martinez, T. J.; Aluru, N. R.; White, S. R.; Sottos, N. R. *J. Appl. Phys.* **2013**, *114*, 023504.
- (30) Silberstein, M. N.; Cremar, L. D.; Beiermann, B. A.; Kramer, S. B.; Martinez, T. J.; White, S. R.; Sottos, N. R. *J. Mech. Phys. Solids* **2014**, *63*, 141–153.
- (31) Atkin, P.; de Paula, J. *Atkins' Physical Chemistry*, 7th ed.; Oxford University Press, 2002.
- (32) Smets, G. *Photochromic Phenomena in the Solid Phase*; Advances in Polymer Science; Springer-Verlag: Berlin/Heidelberg, 1983; Vol. 50, pp 17–44.
- (33) Silberstein, M. N.; Cremar, L. D.; Beiermann, B. A.; Kramer, S. B.; Martinez, T. J.; White, S. R.; Sottos, N. R. *J. Mech. Phys. Solids* **2014**, *63*, 141–153.
- (34) Beiermann, B. A.; Kramer, S. L. B.; Moore, J. S.; White, S. R.; Sottos, N. R. *ACS Macro Lett.* **2012**, *1*, 163–166.
- (35) Evans, M. G.; Polanyi, M. *Trans. Faraday Soc.* **1935**, *31*, 875.
- (36) Eyring, H. *J. Chem. Phys.* **1935**, *3*, 107.
- (37) Ong, M. T.; Leiding, J.; Tao, H.; Virshup, A. M.; Martinez, T. J. *J. Am. Chem. Soc.* **2009**, *131*, 6377–6379.
- (38) Groote, R.; Szyja, B. M.; Pidko, E. A.; Hensen, E. J. M.; Sijbesma, R. P. *Macromolecules* **2011**, *44*, 9187–9195.
- (39) Eyring, H. *J. Chem. Phys.* **1936**, *4*, 283–291.
- (40) Ward, I. M.; Wilding, M. A. *J. Polym. Sci., Polym. Phys. Ed.* **1984**, *22*, 561–575.
- (41) Kaminski, K.; Pawlus, S.; Adrjanowicz, K.; Wojnarowska, Z.; Włodarczyk, P.; Paluch, M. *J. Phys.: Condens. Matter* **2012**, *24*, 065105.
- (42) Wang, Q.; Gossweiler, G. R.; Craig, S. L.; Zhao, X. *J. Mech. Phys. Solids* **2015**, *82*, 320–344.